



OPEN

Assessment and evolution analysis of urban infrastructure resilience under flood disaster scenarios based on the PSR model and extension catastrophe progression

Chenxin Yang, Zhigang Jin✉ & Hao Yin

As global climate change intensifies and urbanisation continues to advance, cities are facing increasingly severe threats from extreme rainfall and flooding. As the critical infrastructure that supports urban functions, urban infrastructure (UI) is both a target of disasters and a conduit for disaster propagation. This amplifies the impact of disasters on cities. This study is based on flood disasters and combines the PSR model and the mutation series model to construct a comprehensive evaluation index system for the resilience of urban infrastructure under flood disasters. In practical application, the Pearl River Delta was selected as a case study to assess the resilience of its urban infrastructure and explore its temporal evolution and spatial distribution between 2018 and 2023. The research findings indicate that: The following conclusions may be deduced from the data: (1) From 2018 to 2023, the overall resilience of urban infrastructure in the Pearl River Delta region showed an upward trend; (2) Guangzhou and Shenzhen had significantly higher infrastructure resilience levels than other cities in the region; (3) The resilience levels of regions such as Zhaoqing and Jiangmen were relatively low. Drawing upon the United Nations Sustainable Development Goals, this study proffers bespoke recommendations for augmenting the resilience of urban infrastructure in the Pearl River Delta region, thereby providing a theoretical underpinning for the formulation of infrastructure development policies in the region.

Keywords Flood, Urban infrastructure resilience, PSR model, Catastrophe model

As global warming causes temperatures to rise, extreme disasters are on the rise, and floods are occurring frequently around the world¹. According to statistics from the 2023 Global Natural Disaster Assessment Report, flood disasters rank as the most frequent natural disasters, affecting the largest number of people². Floods have a greater impact on urban areas, mainly because flooding disrupts the normal operation of roads, bridges, and other transportation facilities^{3,4}. This will affect residents' normal lives, slow down the availability of emergency services, and impact post-disaster reconstruction capabilities⁵. Therefore, it is of vital importance to systematically assess the impact of floods on urban infrastructure. Engineering infrastructure is generally divided into six major systems: transportation, water supply and drainage, communications, energy supply, urban environment, and disaster prevention⁶. These six systems not only serve residents' daily lives but also support the operation of other infrastructure, collectively forming an open, complex, and dynamic system. Based on this, the urban infrastructure studied in this paper specifically refers to engineering infrastructure.

As an important material foundation for the realization of urban functions and healthy development, the UI plays a crucial role in improving citizens' living conditions, enhancing the city's overall carrying capacity, and increasing the efficiency of urban operations⁷. Once infrastructure systems are unable to withstand adverse shocks, they will trigger a chain reaction, causing immeasurable and serious damage to cities^{8,9}. Recent disasters have demonstrated the importance of UI during urban flooding. For example, in July 2023, persistent heavy rainfall in northern India triggered severe flooding, submerging urban roads and homes and bringing daily life to a standstill. The extreme precipitation overwhelmed city drainage systems, causing rainwater to pool in low-lying areas and create urban flooding. Water inundation damaged electrical infrastructure, triggering

School of Architecture and Civil Engineering, Xihua University, Chengdu 610039, China. ✉email: jinzhigang@xhu.edu.cn

short circuits that led to power outages and subsequently hampered rescue operations^{10,11}. During extreme rainfall events, urban drainage systems become overwhelmed. Rainwater can no longer enter the pipes and begins accumulating in low-lying areas, causing urban flooding. This accumulated water gradually encroaches upon critical city infrastructure, with power systems being particularly vulnerable. When floodwater infiltrates electrical facilities, it causes short circuits, ultimately leading to power outages that hinder rescue operations^{10,11}. Given that enhancing the disaster resilience of urban infrastructure (UI) is fundamental to sustaining normal urban operations^{12,13}, the concept of resilience has become a central focus globally, particularly among global organizations and numerous developed nations. These countries have launched initiatives to promote and implement resilient infrastructure, intending to enhance cities' ability to adapt to disasters¹⁴.

Resilience originated from the concept of elasticity in physics, which refers to a material's capacity to absorb deformation forces when subjected to external forces. It was first applied to academic research by Holloing¹⁵. The adoption of the concept of resilience in multiple fields has led to the expansion of its meaning. The subsystems of the UI are interdependent and collectively support urban operations¹⁶, playing their respective roles at different stages of a disaster and collectively forming the overall resilience of urban infrastructure. Piratla et al.¹⁷ define infrastructure resilience as the ability of a system to withstand pressure and respond to failures. Li¹⁸ defines urban infrastructure resilience as the ability of an infrastructure system to withstand shocks, absorb losses, and quickly return to normal operation during a disaster. In this paper, UI resilience is defined as the ability of UI to resume normal operations after natural disasters.

More scholars are now considering the impact of extreme weather on UI alongside their UI research. Saiful Arif Khan¹⁹ proposed an integrated framework combining the Dempster-Shafer method and the best-worst method to analyze the resilience of bridge infrastructure under earthquake disasters. Sun²⁰ introduced the comprehensive concept of resilience in flood disaster research, considering both natural environmental and socio-economic factors, and implemented integrated management across pre-disaster, during-disaster, and post-disaster stages to achieve an accurate assessment of flood disaster resilience. Ambily²¹ measures the flood resilience of urban blue-green infrastructure using the ecological flood index, conducting a comprehensive analysis of urban flood resilience in areas ranging from "very low" to "extremely low," thereby facilitating a transition from risk management to resilience management for urban floods. Seyed²² studied how well road networks perform when there are different disaster scenarios. This was done by using a system that looks at how well different things work. The study also looked at how strong road networks are against floods. Therefore, exploring how to apply flood resistance capabilities can effectively strengthen flood management and reduce the impact of floods on cities. However, most scholars currently focus on studying individual UI systems, with limited attention to the overall UI system; additionally, few studies integrate urban flood disasters with the overall resilience of UI systems.

Resilience theory is still in its early stages of development in the field of urban infrastructure, with relatively vague concepts, unclear data processing standards, and numerous theoretical frameworks that are difficult to unify. Additionally, existing disaster resilience assessment methods generally suffer from limitations in applicability and strong subjectivity²³, while non-model assessment methods are constrained by poor generalization capabilities²⁰. The aforementioned factors serve to compound the complexity inherent in resilience assessment. It is evident that, should these issues remain unresolved, they will have a significantly detrimental effect on the development and promotion of resilience theory for infrastructure in the context of flood disasters. Catastrophe theory is a general theoretical method that has been specifically designed to represent changes in system states²⁴. It reflects the system's state, with different model positions representing significantly distinct meanings²⁵. Catastrophe theory has the potential to function as an unbiased, widely applicable approach for formulating and advocating for the development and promotion of UI resilience theory.

In resilience assessment analysis, the most significant difference lies in whether a model is used. Semi-Markov models have advantages in quantifying system state transitions and residence times²⁶, but they are less capable of analyzing the overall performance of system resilience. The judgment matrices in AHP and the training sets in supervised learning models rely on expert knowledge or subjective judgments²⁷, which introduces subjective factors into the assessment and affects the accuracy of model judgments. Given that UI resilience encompasses multifaceted and wide-ranging dimensions, its evaluation framework should align with the interconnected structure of systems and the adaptive characteristics of risk management. The Pressure-State-Response model comprehensively considers various factors influencing the environment^{28,29} and integrates these factors organically for analysis, thereby providing decision-makers with a systemic perspective^{30,31}.

The innovations of this paper are as follows: Firstly, the present study focuses on the theoretical construction and methodological innovation of urban infrastructure resilience under flood disasters. The present study addresses the current weaknesses in systematic response mechanisms within disaster prevention and mitigation systems, as well as the lack of in-depth theoretical elaboration on urban infrastructure resilience in existing research. To address these issues, a resilience assessment framework integrating multidimensional indicators is constructed. This development serves to broaden the methodological approach for integrating disaster research with resilience theory. Secondly, in order to address the bias arising from subjective weighting in extant evaluation methods (e.g., AHP, TOPSIS), the disaster progression method is introduced. This approach is predicated on the premise that weights are determined based on intrinsic mathematical relationships among indicators, thereby enhancing the objectivity and robustness of the assessment. Thirdly, the study goes beyond the evaluation of urban infrastructure resilience during flood disasters. It further analyzes the spatio-temporal evolution of resilience using the Moran index. The text explores comprehensive development strategies for cities in the Pearl River Delta from multiple perspectives, providing policy recommendations for integrated regional urban development. The following essay will provide a comprehensive overview of the relevant literature on the subject.

Overview of the research area

The Pearl River Delta is located in southern China, comprising the country's largest river system and most developed region. The area is characterized by low-lying terrain and high population density, making it highly susceptible to flood disasters^{32,33}. Since the twenty-first century, the Pearl River Delta has primarily exhibited riverine alluvial and sedimentary processes, accompanied by frequent flood events. River water levels fluctuate significantly, annual precipitation is high, and the region is strongly influenced by monsoon climate patterns. Changes in water levels and flood frequencies along the Pearl River mainstem and its tributaries have a particularly significant impact on surrounding areas.

The present study has focused on the Pearl River Delta region, with specific reference to the cities of Guangzhou, Shenzhen, Zhuhai, Foshan, Dongguan, Zhongshan, Jiangmen, Zhaoqing, and Huizhou. These cities have all suffered severe flood disasters and are representative in terms of geographical distribution and disaster intensity. This research aims to analyse the causal mechanisms, spatial distribution characteristics, and socio-economic impacts of flood disasters in the Pearl River Delta region in depth, thereby providing a scientific basis for regional disaster prevention and mitigation efforts. The specific geographical locations of the study areas are illustrated in Fig. 1.

Indicator system construction and research methods

In consideration of the fact that the Pearl River Delta is a region of China that is subject to frequent flooding, it is imperative to undertake a comprehensive study of the UI in the Pearl River Delta region that has been impacted by floods. Firstly, the PSR model proposed by Canadian statisticians David J. Rapport and Tony Friend³⁴ was employed to construct an indicator system, with three aspects being taken into consideration: pressure, state, and response. Secondly, the entropy weight method is employed to objectively and scientifically determine the weights of each indicator. Based on catastrophe theory, the catastrophe series method is used to calculate the resilience of urban infrastructure. Subsequently, ArcGIS software is utilized to spatially map the resilience of UI across cities in the Pearl River Delta; furthermore, layers are imported into GeoDa software to analyse the spatial global and local correlations of the case study.

Construction of indicator systems and data sources

In consideration of the fact that the present study is concerned with flood disasters, the disaster data primarily encompasses flood-related events. However, it is important to note that the scope of the resilience survey can be

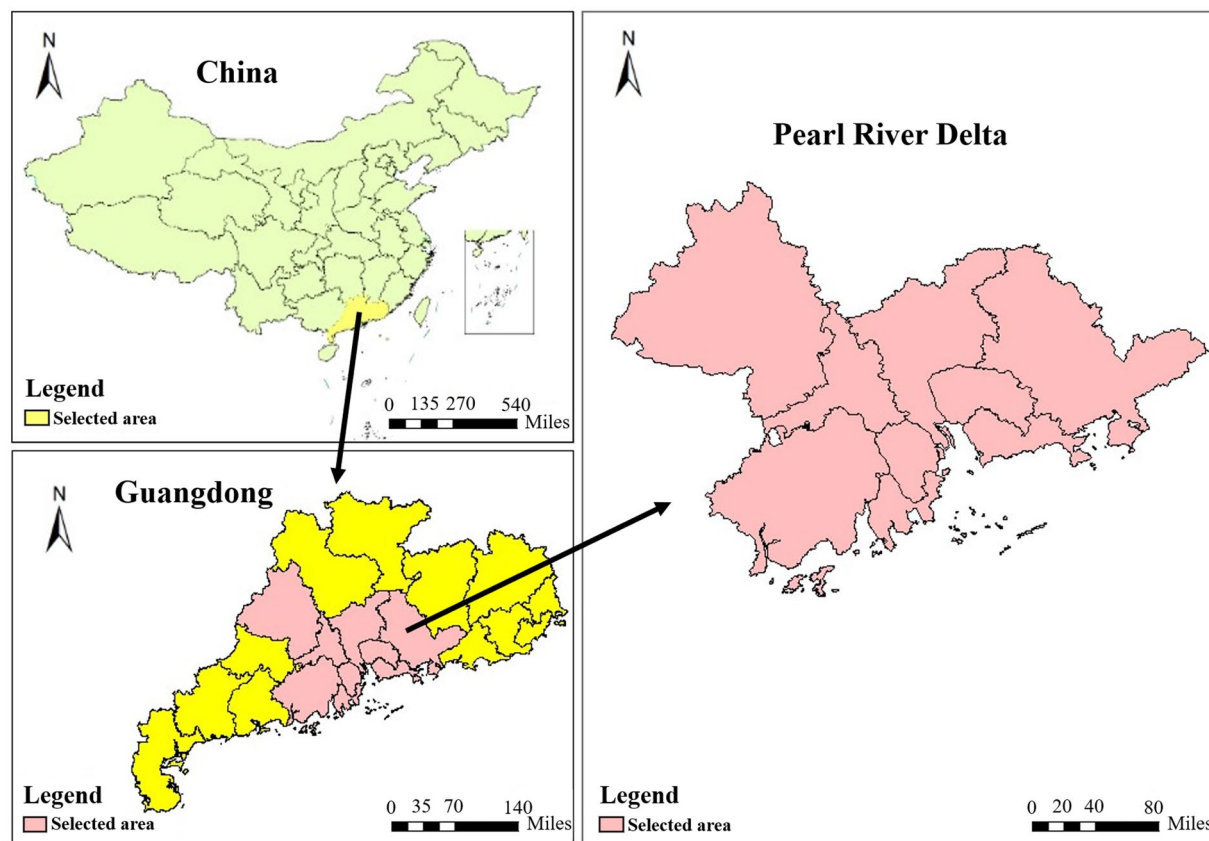


Fig. 1. Spatial distribution of the Pearl River Delta in the study area. The base map was obtained from DataV Data Visualization Platform. (https://datav.aliyun.com/portal/school/atlas/area_selector), and the maps were generated using ArcGIS 10.8.1 (<https://enterprise.arcgis.com/zh-cn/>).

expanded to encompass any disaster category. The data utilised in this study encompasses a range of dimensions, including natural disasters, population distribution, environmental issues, and social security. With regard to the selection of indicators, a systematic review of the relevant literature was conducted, field research was carried out, and the characteristics of flood disasters in urban areas were analysed in depth. The construction of a comprehensive evaluation indicator system was finally achieved, comprising three dimensions: pressure, state, and response. The term “pressure” is used to denote the threats and disruptions caused by natural disasters to urban infrastructure, while “state” refers to the resilience of UI to flood disasters under pressure conditions. The term “response” is employed to denote the recovery capacity of UI in the context of flood disasters. The data utilised in this study is predominantly comprised of vector data and panel data. The missing data were supplemented using linear interpolation methods. The primary data sources comprise the National Population Census, municipal statistical yearbooks, and government official websites. Table 1 provides specific indicator information and the rationale behind their selection.

Determination of indicator weights

The entropy weight method constitutes an objective weighing method insofar as its weights are determined exclusively based on the intrinsic information of the data. By virtue of this, human subjective preferences and

General objectives	Dimension	Primary indicator	Secondary indicators	Description
Urban infrastructure resilience	A Stress resilience	A1 Rainfall and human activity conditions	A11 Annual average daily rainfall	Higher rainfall increases stress on urban infrastructure (-)
			A12 Population density	Higher population density increases pressure on urban resources (-)
		A2 Topography and rivers	A21 Elevation	Higher elevation favors higher urban flooding capacity (+)
			A22 Slope orientation	Reasonable slope setting can utilize gravity to enhance urban drainage capacity (+)
			A23 Slope	The greater the slope, the greater the urban drainage capacity (+)
			A24 River density	A high-density river network means that more of the city's infrastructure is directly exposed to the river and its floodplain reach (-)
		B1 Energy supply	B11 Natural gas supply capacity	Natural gas supply is able to secure basic livelihood needs and improve the overall resilience of the city in the event of flooding (+)
			B12 Power supply capacity	In the face of flood disasters, enhanced power supply capabilities can improve energy access and living standards (+)
			B13 Electricity consumption per capita	Higher per capita electricity consumption leads to greater challenges for urban infrastructure (-)
		B2 Water supply and drainage treatment	B21 Integrated water supply generation capacity	The stronger the comprehensive water supply generation capacity, the stronger the city's water supply capability, and the faster the recovery from flood disasters (+)
			B22 Urban sewage treatment rate	The higher the sewage treatment rate, the stronger the city's resilience against urban flooding and backflow (+)
			B23 Density of drainage pipe network	The greater the density of the drainage network, the greater the city's flood relief capacity (+)
		B3 Transportation operational capacity	B31 Highway density	High highway density ensures that accessible routes remain between points within the city, accelerating the recovery process after disasters (+)
			B32 Density of public transportation coverage	A high-density public transit network can help cities absorb the impact of flood disasters and maintain essential mobility at the minimum level (+)
			B33 Cargo turnover capacity	High cargo turnover capacity ensures that vital supplies can continue flowing to where they are needed during flood disasters (+)
		B4 Communication capacity	B41 Number of cell phone subscribers	Cell phones can provide disaster alerts and related information (+)
			B42 Number of Internet broadband access	The internet can help residents access information about flood disasters (+)
	C Response Resilience	C1 Funding and staffing	C11 Level of local fiscal tax revenues	Local fiscal revenues can affect response capacity and the speed of disaster recovery (+)
			C12 Economic density	Economic density affects the speed of a city's recovery after a disaster (+)
			C13 Employment level in the electricity, heat, gas, water production and supply industry	When cities face flood disasters, personnel at the operational level make real-time decisions and perform emergency maintenance on urban infrastructure to mitigate the impact of floods on the city (+)
			C14 Level of employed persons in the water conservancy, environment and public facilities management industry	
		C2 Capacity of medical institutions	C21 Number of health technicians per 10,000 people	The more health technicians, the stronger the rescue capacity (+)
			C22 Number of beds in health institutions per 10,000 people in the city	Health institutions can provide medical services to urban disaster victims (+)
		C3 Research investment	C31 Full-time equivalent level of R&D personnel	The higher the full-time equivalent level of R&D personnel, the stronger a city's technological innovation and R&D capabilities become, and the greater its resilience, absorption capacity, and recovery capability in the face of flood disasters (+)
			C32 R&D Funding Input Level	The higher the level of R&D funding, the greater the impetus for technological innovation, systematically enhancing a city's capacity to respond to floods and waterlogging (+)

Table 1. UI resilience indicator system.

experiential judgments are avoided³⁵. Consequently, this renders the results more persuasive. The present paper employs the entropy weight method to calculate the weights of UI resilience indicators under flood disasters. The following specific steps are to be taken:

(1) Establishing the evaluation matrix.

To mitigate the influence of inconsistent measurement units across the dataset, this study applies formula (1) to standardize the data, thereby converting all indicator values to the range [0,1]. The specific normalization formula is shown below:

$$Z_{ij} = \frac{r_{ij} - \min(r_{ij})}{\max(r_{ij}) - \min(r_{ij})}, \text{ for positive indicators} \quad (1)$$

$$Z_{ij} = \frac{\max(r_{ij}) - r_{ij}}{\max(r_{ij}) - \min(r_{ij})}, \text{ for negative indicators}$$

where Z_{ij} represents the original matrix, and Z represents the normalization matrix.

Initially, the weight of each indicator must be calculated based on standardized data, employing formula (2). Subsequently, the application of information entropy theory should be undertaken in order to calculate the information entropy of each indicator, with formula (3) being utilized for this purpose. Thereafter, formula (4) should be employed to determine the weight of the indicator based on the entropy value. Finally, the calculated weight must be applied to the normalization matrix using formula (5).

$$P_{ij} = \frac{z_{ij}}{\sum_{i=1}^n z_{ij}}, (j = 1, 2, \dots, m) \quad (2)$$

$$E_j = -\frac{\sum_{i=1}^n P_{ij} \ln P_{ij}}{\ln n}, (j = 1, 2, \dots, m) \quad (3)$$

$$w_j = \frac{1 - E_j}{\sum_{j=1}^m (1 - E_j)} \quad (4)$$

$$x_{ij} = w_j \times z_{ij} \quad (5)$$

In this formula, P_{ij} denotes the proportion of the standardized values of each city under the indicator, E_j represents information entropy, and x_{ij} represents the weighted standardized matrix. The weighting results calculated by employing the entropy-based weighting method are presented in Table 2.

The research investment indicator data in the entropy weighting method is sourced from the Guangdong Statistical Yearbook (2018–2023). The disproportionately high weight assigned to research investment stems from Shenzhen's significantly greater R&D expenditure compared to most cities in the Pearl River Delta region. This disparity arises because Shenzhen ranks among China's three major financial centres³⁶, and stands as one of the most critical hubs for scientific and technological innovation in the country and globally³⁷. Scientific research can significantly enhance the quality and efficiency of urban infrastructure³⁸, promote the digital transformation of urban infrastructure³⁹, and consequently improve a city's resilience to disasters⁴⁰.

Mutation series method

The selection of evaluation methods requires discernment of their core characteristics and applicable scenarios. The present study focuses on the assessment of the resilience of urban infrastructure during flood disasters, to select analytical tools that best align with research objectives and data characteristics. Table 3 provides a comparative overview of six evaluation methods.

The selection of catastrophe theory for this study is also justified by the following reasons: (1) The framework of catastrophe theory is systematic⁴¹, and can be integrated with the PSR model to comprehensively cover all aspects of urban infrastructure resilience assessment under flood disasters. (2) The analytical approach grounded in catastrophe theory is methodical⁴², enabling clear evaluation of complex urban infrastructure resilience indicator systems. (3) Catastrophe models exhibit "lagging" characteristics⁴³, allowing more precise assessment of trends in urban infrastructure resilience under flood disasters.

The core of catastrophe theory lies in revealing how minute changes in environmental conditions trigger abrupt transitions from continuous quantitative changes to discontinuous qualitative changes in systems⁴⁴. Common catastrophe models include the collapse, sharp-head, swallowtail, and butterfly models. These are respectively applicable to different numbers of control variables and varying levels of system complexity⁴⁵.

(1) Classification of mutation models.

Following the completion of the dimensionless calculation of the original indicator data, various objects and factors are conceptualised as state and control variables. State variables are typically comprised of multiple control variables⁴⁶. It is assumed that the target of the framework is the state variable. In this case, the control variable is representative of the sub-indicators it contains. The model with two sub-indicators is known as the spike mutation model. The models and normalization formulas are shown in Table 4 below: Calculate the mutation level values of different needle grades using the corresponding matching mutation models based on the normalization formulas.

General objectives	Dimension	Weighting	Primary indicator	Weighting	Secondary indicators	Weighting	Sort	
Urban infrastructure resilience	A Stress resilience	0.143	A1 Rainfall and human activity conditions	0.018	A11 Annual average daily rainfall	0.007	24	
					A12 Population density	0.011	15	
		0.143	A2 Topography and rivers	0.124	A21 Elevation	0.05	4	
					A22 Slope orientation	0.02	16	
	B state resilience	0.343		0.067	A23 Slope	0.031	9	
					A24 River density	0.023	15	
		B1 Energy supply			B11 Natural gas supply capacity	0.024	13	
		0.343		0.067	B12 Power supply capacity	0.031	8	
					B13 Electricity consumption per capita	0.012	22	
	C Response resilience	0.514	B2 Treatment of water supply and drainage	0.067	B21 Integrated water supply generation capacity	0.026	10	
					B22 Urban sewage treatment rate	0.006	25	
					B23 Density of drainage pipe network	0.035	7	
			B3 Transportation operational capacity	0.156	B31 Highway density	0.017	18	
					B32 Density of public transportation coverage	0.017	19	
					B33 Cargo turnover capacity	0.122	3	
			B4 Communication capacity	0.052	B41 Number of cell phone subscribers	0.015	21	
					B42 Number of Internet broadband access	0.038	5	
			C1 Funding and staffing	0.096	C11 Level of local fiscal tax revenues	0.036	6	
					C12 Economic density	0.016	20	
					C13 Employment level in the electricity, heat, gas, water production and supply industry	0.02	17	
					C14 Number of employees in the water conservancy, environmental protection, and public facilities management industry	0.025	12	
			C2 Capacity of medical institutions	0.048	C21 Number of health technicians per 10,000 people	0.025	11	
					C22 Number of beds in health institutions per 10,000 people in the city	0.024	14	
			C3 Research investment	0.37	C31 Full-time equivalent level of R&D personnel	0.195	1	
					C32 R&D Funding Input Level	0.175	2	

Table 2. The weights were calculated by means of the entropy weight method.

Evaluation method	Advantages	Limitations	Scope of Application
Analytic hierarchy process (AHP)	Clear structure and strong systematic approach; Capable of integrating quantitative and qualitative indicators	Highly subjective; consistency testing becomes cumbersome with numerous indicators	Suitable for constructing evaluation indicator systems for infrastructure resilience and determining the relative importance of each dimension. Suitable for pre-disaster resilience capability assessment and planning
ANP network analysis	Capable of handling complex feedback and dependency relationships, making it more practical	Highly complex to operate, computationally intensive, and heavily reliant on software and expert judgment	ANP is an ideal choice if this study aims to analyze the complex interactions and feedback mechanisms among flood resilience evaluation indicators (e.g., exposure, vulnerability, adaptive capacity). However, its application incurs high costs (time and manpower)
TOPSIS	Fully data-driven with strong objectivity	Weights represent information content rather than actual importance, potentially leading to distortion	Suitable for this study to precisely rank and categorize the infrastructure resilience levels of multiple cities in the Pearl River Delta after determining indicator weights. This method clearly illustrates each city's gap relative to the ideal resilience level
Grey relational analysis (GRA)	Low data requirements; analyzable with small samples; simple underlying principle	Highly subjective (sensitive to the selection of correlation coefficient ρ); limited theoretical depth	If evaluation data is limited or partially missing in this study, GRA can serve as an effective supplementary analytical tool for preliminary identification of key factors affecting infrastructure resilience or for trend analysis

Table 3. Analysis of advantages, disadvantages, and applicability of primary evaluation methods in this study.

	State variables	Control variables	Potential function	Normalization formula
Pointed type	1	2	$f(x) = x^4 + ax^2 + bx$	$x_a = a^{\frac{1}{2}}, x_b = b^{\frac{1}{3}}$
Swallowtail type	1	3	$f(x) = x^5 + ax^3 + bx^2 + cx$	$x_a = a^{\frac{1}{2}}, x_b = b^{\frac{1}{3}}, x_c = c^{\frac{1}{4}}$
Butterfly type	1	4	$f(x) = x^6 + ax^4 + bx^3 + cx^2 + dx$	$x_a = a^{\frac{1}{2}}, x_b = b^{\frac{1}{3}}, x_c = c^{\frac{1}{4}}, x_d = c^{\frac{1}{5}}$

Table 4. Mutation system model and normalization formula.

Indicator hierarchy	Indicators within hierarchy	Internal relationships
Dimension	A, B, C	Complementary
Primary indicators	A1, A2	Complementary
	B1, B2, B3, B4	Complementary
	C1, C2, C3	Complementary
Second-level indicators	A11, A12	Complementary
	A21, A22, A23, A24	Complementary
	B11, B12, B13	Complementary
	B21, B22, B23	Complementary
	B31, B32, B33	Non-complementary
	B41, B42	Non-complementary
	C11, C12, C13, C14	Non-complementary
	C21, C22	Complementary
	C31, C32	Complementary

Table 5. Relationships among secondary indicators.

Mutation model	Control the relationship between variables	
	Non-complementary	Complementary
Pointed type	$\min(x_a, x_b)$	$(x_a, x_b)/2$
Swallowtail type	$\min(x_a, x_b, x_c)$	$(x_a, x_b, x_c)/3$
Butterfly type	$\min(x_a, x_b, x_c, x_d)$	$(x_a, x_b, x_c, x_d)/4$

Table 6. Determination of mutation rate values.

In the potential function of the aforementioned mutation model, the independent variable x represents the state variable. The function $f(x)$ is referred to as the potential function of the independent variable x . The coefficients a , b , c , and d serve as control parameters that govern the independent variable x .

(2) Evaluation using the normalization formula.

When evaluating using normalization formulas, the values of state variables should be calculated for each control variable, adhering to two key principles. The “non-complementarity” principle governs calculations where control variables lack clear interrelationships (non-complementary indicators), employing the “minimizing the larger value” approach for calculating sudden change levels⁴⁷. Conversely, when significant correlations exist among control variables⁴⁷, the “complementarity” principle mandates using the average value of state variables. Through multiple rounds of consultation and workshops with domain experts, this paper establishes the internal logical relationships and overall structural integrity of the urban infrastructure resilience indicator evaluation system under flood disasters. The relationships among secondary indicators are shown in Table 5.

Based on the normalization formula, indicator weighting, and indicator relationship principles, the final mutation level value is derived. The formula is shown in Table 6.

Interval partitioning

After obtaining preliminary evaluation results based on catastrophe models, interval partitioning methods are often employed to refine and categorize these outcomes. Unlike traditional evaluation methods that struggle to effectively process large-scale, high-dimensional data, the K-means clustering algorithm—a classic unsupervised learning algorithm—automatically aggregates similar samples into clusters based on intrinsic data characteristics without requiring predefined category labels. This approach reduces the interference of subjective judgments in the evaluation process, enhancing the objectivity and scientific rigor of resilience level classification⁴⁸.

The steps of the K-means clustering algorithm are as follows: (1) Randomly select k cluster centers, (2) Assign each data point to its nearest cluster center, (3) Recalculate the mean of each cluster as the new center, (4) Iterate this process until the cluster centers remain unchanged⁴⁹.

Applying the K-means clustering algorithm enables the division of urban infrastructure resilience evaluation results under flood disasters into multiple intervals, allowing for sequential analysis of each independent interval.

Spatial correlation evolution analysis method

Spatial weighting

This study employs the spatial analysis software GeoDa to investigate the spatial correlation among urban infrastructure resilience levels during flood disasters. GeoDa primarily provides four types of spatial weight

matrices: Queen adjacency, Rook adjacency, Threshold distance, and K-Nearest neighbors. The definitions, advantages, and disadvantages of various spatial weight matrices are shown in Table 7.

The Pearl River Delta was selected as the study area. When examining the resilience of its urban infrastructure, Queen Contiguity more effectively captures the proximity of areas separated only by a river. It treats areas sharing a vertex—such as bridge junctions or road intersections—as neighbors, aligning more closely with the reality of “seamless connections” among cities in the Pearl River Delta. This approach better reflects the macro-level spatio-temporal distribution relationships. Therefore, constructing a spatial weight matrix of the Queen Contiguity type is more appropriate for exploring the spatial correlations of urban infrastructure resilience in the Pearl River Delta.

Moran's I index

The present study employs Moran's I global spatial econometric model to reflect the global autocorrelation spatial relationship of urban flood disaster resilience. The calculation formula is as follows:

$$\text{Global Moran}' sI = \frac{\sum_{i=1}^n \sum_{j=1}^n W_{i,j} Z_i Z_j}{S^2 \sum_{i=1}^n \sum_{j=1}^n W_{i,j}} \quad (6)$$

$$S^2 = \frac{1}{n} \sum_{i=1}^n Z_i^2 \quad (7)$$

Among these, Z_i represents the difference between the urban infrastructure flood resilience index and the average flood resilience index of all urban infrastructure in the study area, while $W_{i,j}$ denotes the spatial weight of urban infrastructure flood resilience in the study area, with a value of 1 for spatially adjacent areas and 0 for non-adjacent areas. The Z_I score is calculated as follows:

$$Z_I = \frac{1 - E(I)}{\sqrt{V(I)}} \quad (8)$$

$$\text{Among them } E(I) = -\frac{1}{n-1}; V(I) = E(I^2) - E(I)^2$$

Due to the unique characteristics of the study area, the constructed Queen Contiguity spatial weight matrix may exhibit “neighbor shortage” in peripheral regions, while central areas demonstrate better representativeness. Therefore, Local Moran's I was employed to supplement these limitations, thereby preventing global indicators from obscuring peripheral regions.

The Local Index of Spatial Association (LISA) is a tool that can be utilized to reflect the spatial correlation between a given geographic unit and its neighboring regions. A frequently employed local index of spatial association is the local Moran's I:

$$\text{Local Moran}' sI = \frac{Z_i}{S^2} \sum_{j \neq i}^n W_{i,j} Z_j \quad (9)$$

The Local Moran's I index has been utilized to categorize the spatial association patterns within the study region into four specific categories: (1) areas with high values surrounded by high values (HH clusters), (2) areas with high values adjacent to low values (HL outliers), (3) areas with low values neighbouring high values (LH outliers), and (4) areas with low values surrounded by low values (LL clusters). The visualization of these spatial autocorrelation patterns can be most effectively achieved through the use of LISA cluster maps.

Matrix type	Definition	Advantages	Disadvantages
Queen adjacency	Two spatial units are considered neighbors if they share any length of common boundary (edge) or vertex	Simple and intuitive, suitable for most polygonal data	May result in many cells having numerous neighbors (e.g., large polygons) or some cells having no neighbors (island problem)
Rook adjacency	Two spatial units are considered neighbors if they share a common edge (not just a vertex)	This is stricter than the Queen definition, excluding cases connected solely by vertices	Uneven neighbor counts and island problems may still occur
Threshold distance	Set a threshold distance (d). If the distance between the centers of mass of two units is less than or equal to this distance, they are considered neighbors	Highly flexible, suitable for irregular units; ensures all units have at least some neighbors	The choice of threshold distance d is subjective; it may result in global connectivity (all cells are neighbors) or local connectivity imbalance
K-Nearest neighbors	Identifies the K nearest neighboring cells for each spatial cell	Effectively addresses uneven neighbor counts by guaranteeing each cell has the same number of neighbors; particularly suitable for datasets with highly variable cell sizes	May result in asymmetric neighbor relationships (i is a neighbor of j, but j is not necessarily a neighbor of i), though GeoDa typically symmetrizes these relationships

Table 7. Definition, advantages and disadvantages of the spatial weight matrix.

Interval	(0, 0.8365]	(0.8365, 0.8751]	(0.8751, 0.9015]	(0.9015, 0.9329]	(0.9329, 1)
Rating grade	Low	Lower	Medium	Higher	High

Table 8. Urban infrastructure rating grade intervals.

2018			2019			2020		
Region	Evaluation results	Resilience level	Region	Evaluation results	Resilience level	Region	Evaluation results	Resilience level
Guangzhou	0.9161	Higher	Guangzhou	0.9179	Higher	Guangzhou	0.9207	Higher
Foshan	0.8734	Lower	Foshan	0.8766	Medium	Foshan	0.8625	Lower
Zhaoqing	0.8834	Medium	Zhaoqing	0.8818	Medium	Zhaoqing	0.8717	Lower
Dongguan	0.8458	Lower	Dongguan	0.8681	Lower	Dongguan	0.8881	Medium
Huizhou	0.9053	Higher	Huizhou	0.8968	Medium	Huizhou	0.9015	Higher
Zhuhai	0.9038	Higher	Zhuhai	0.9079	Higher	Zhuhai	0.9082	Higher
Zhongshan	0.8746	Lower	Zhongshan	0.866	Lower	Zhongshan	0.8722	Lower
Jiangmen	0.9017	Higher	Jiangmen	0.9041	Higher	Jiangmen	0.904	Higher
Shenzhen	0.9024	Higher	Shenzhen	0.9288	Higher	Shenzhen	0.9301	High
2021			2022			2023		
Guangzhou	0.9238	Higher	Guangzhou	0.9264	Higher	Guangzhou	0.9263	Higher
Foshan	0.8737	Lower	Foshan	0.8704	Lower	Foshan	0.8713	Lower
Zhaoqing	0.8838	Medium	Zhaoqing	0.8593	Lower	Zhaoqing	0.8779	Medium
Dongguan	0.8925	Medium	Dongguan	0.891	Medium	Dongguan	0.8862	Medium
Huizhou	0.9005	Medium	Huizhou	0.9025	Higher	Huizhou	0.8964	Medium
Zhuhai	0.9075	Higher	Zhuhai	0.9062	Higher	Zhuhai	0.8943	Medium
Zhongshan	0.8727	Lower	Zhongshan	0.8738	Lower	Zhongshan	0.8785	Medium
Jiangmen	0.9039	Higher	Jiangmen	0.9017	Higher	Jiangmen	0.887	Medium
Shenzhen	0.9412	High	Shenzhen	0.9416	High	Shenzhen	0.9399	High

Table 9. Infrastructure resilience assessment results for cities in the Pearl river delta from 2019 to 2023.

Results and analysis

UI resilience analysis

The entropy weight method is utilised in this study to ascertain the weights of each indicator. Following standardisation and weighting of the initial resilience assessment matrix, the mutation series method is employed to calculate the resilience values of each city in the Pearl River Delta for the pressure-state-response dimension on an annual basis. The specific values are illustrated in the accompanying figure.

This study utilized SPSS Statistics 27 software for K-means clustering analysis, with the infrastructure resilience values of cities in the Pearl River Delta from 2018 to 2023 as clustering factors, to determine the evaluation results and resilience levels of UI resilience. Following the requisite iteration, the cluster centres were obtained, as illustrated in Tables 8 and 9.

The results show that the overall resilience of UI in the Pearl River Delta under flood disasters has been on an upward trend. During the period from 2018 to 2023, although Guangzhou's resilience has been slowly declining, its lowest resilience score remained above 0.91, making it a highly resilient city. Zhaoqing, Foshan, Zhongshan, and Huizhou exhibited fluctuating resilience trends; Dongguan and Shenzhen saw continuous growth in resilience. Overall, the gap in resilience capabilities between regions is gradually narrowing, primarily because Guangzhou and Shenzhen, as core cities of the Pearl River Delta, are driving the development of surrounding cities, particularly in terms of UI construction.

Spatial evolution analysis of UI resilience

In terms of spatial analysis, the present research employed ArcGIS 10.6 and GeoDa 1.2 software platforms to perform the analytical tasks. Specifically, the investigation incorporated the authorised 2024 reference cartographic materials issued by China's national land and resources regulatory body, along with regional topographic maps of the Pearl River Delta and urban safety capacity evaluation metrics, to establish a geospatial analysis framework assessing the infrastructural adaptive capacity of the nine metropolitan areas within the Pearl River Delta urban agglomeration.

Spatial distribution analysis

- (1) Spatial distribution characteristics of urban infrastructure resilience assessment results under flood disasters.

Based on the pressure-state-response GIS model of nine regions in the Pearl River Delta from 2018 to 2023, the pressure-state-response resilience-level-division interval was imported into ArcGIS software. As shown in Fig. 2.

As shown in Fig. 2, the highest values of UI resilience under flood disasters are concentrated in Guangzhou and Shenzhen. This disparity primarily stems from China's significant fiscal investments in these cities and their national strategic status, enabling a four-dimensional synergy of economy, policy, technology, and governance. Overall, coastal cities exhibit generally higher infrastructure resilience, while prefecture-level cities within the region generally have lower resilience. Developed cities drive improvements in infrastructure resilience in surrounding areas, particularly through industrial radiation, infrastructure sharing, and administrative coordination. In terms of industrial radiation, Shenzhen's high-tech industries have expanded eastward to Dongguan and Huizhou, driving industrial chain upgrades and enhancing the resilience of their infrastructure (such as power and transportation). In terms of infrastructure sharing, the extension of the Shenzhen Metro to Dongguan and the Guangzhou Metro to Huizhou directly enhances the resilience of transportation infrastructure in both regions. Additionally, Shenzhen's emergency management system covers Dongguan and Huizhou, establishing a joint prevention and control mechanism. In terms of administrative coordination, Shenzhen, Dongguan, and Huizhou have established a cooperative mechanism within an economic circle to advance cross-city infrastructure projects, such as the Shenzhen-Shanwei High-Speed Railway and the Dongjiang Water Resource Allocation Project, thereby enhancing overall disaster resilience and strengthening the resilience of urban infrastructure. Meanwhile, the radiation effect of developed cities on surrounding cities follows a "core-periphery" model, with the intensity of influence decreasing exponentially with increasing distance.

Spatial correlation analysis

Given that spatial analysis demands macro-scale and quantitative methodologies to unveil spatial spillover effects and agglomeration characteristics, it is imperative to integrate spatial correlation analysis into the research framework to achieve a comprehensive understanding of the spatial distribution patterns of urban infrastructure resilience in the Pearl River Delta region. This analysis should encompass both global and local spatial correlation, thereby facilitating a multifaceted examination of the subject.

(1) Global correlation analysis.

As shown in Table 10, the P-values for all years are less than 0.1, corresponding to Z-scores greater than 1.65, indicating that Moran's I is significant for all years. However, the significance shows an upward trend from 2018 to 2019, begins to decline in 2019, and then increases annually from 2021 to 2023. The changes in Moran's I reflect the spatial clustering pattern of flood resilience in Yangtze River Delta cities over the past six years. All years have positive Moran's I values, indicating that the UI resilience indices of the nine regions in the Pearl River Delta exhibit spatial clustering phenomena. Specifically, regions with high resilience values tend to cluster with neighbouring high-value regions, while regions with low resilience values cluster with other low-value regions, forming a spatial positive correlation pattern.

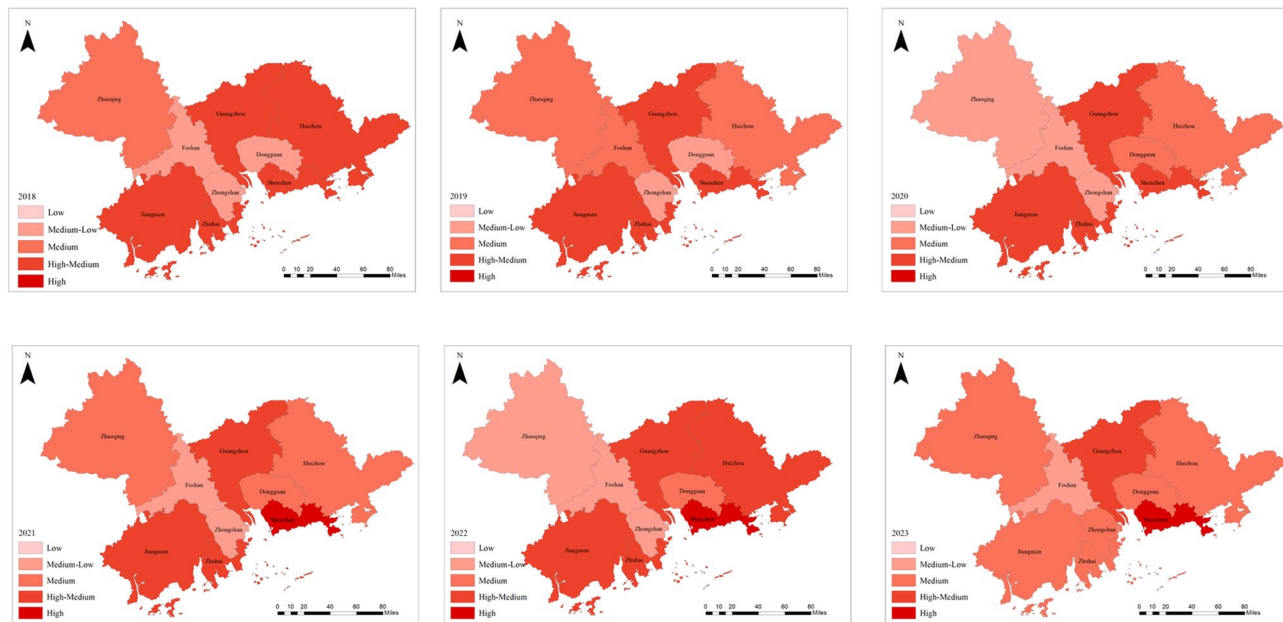
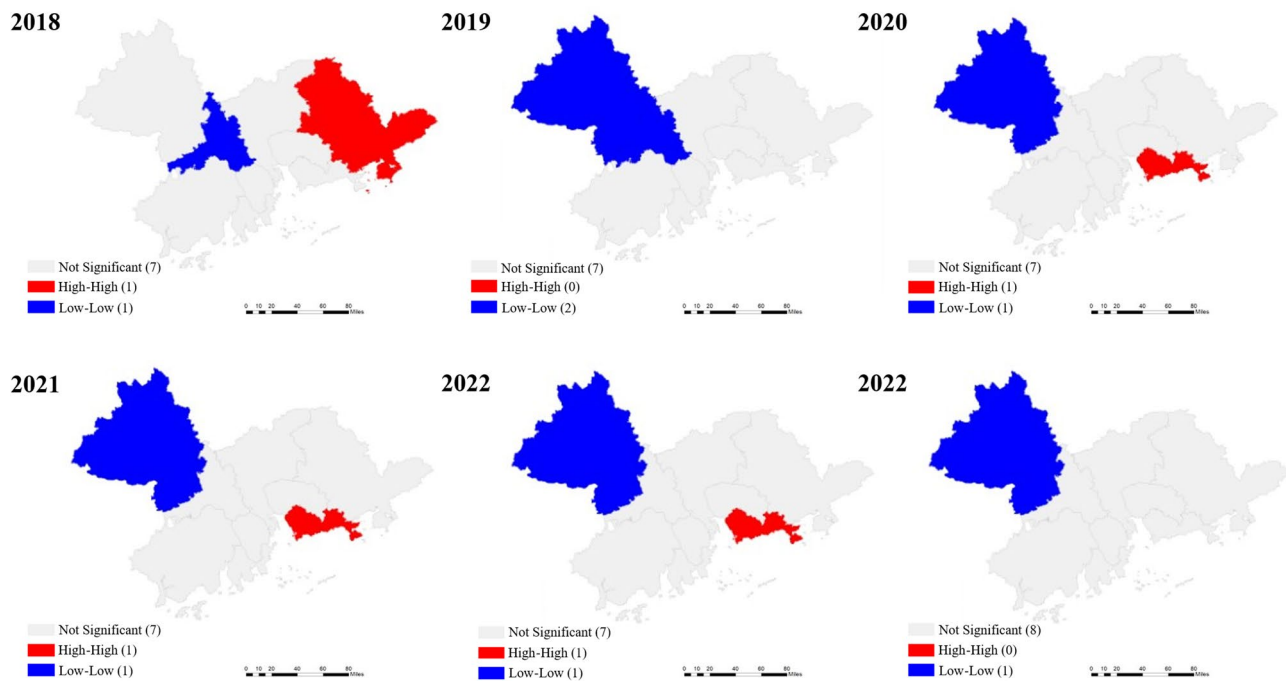


Fig. 2. Spatial distribution of UI resilience in the Pearl River Delta. The base map was obtained from DataV Data Visualization Platform (https://datav.aliyun.com/portal/school/atlas/area_selector), and the maps were generated using ArcGIS 10.8.1 (<https://enterprise.arcgis.com/zh-cn/>).

Year	2018	2019	2020	2021	2022	2023
Moran's I Index	0.477	0.5311	0.6327	0.556	0.4605	0.2316
Z score	2.8992	2.7642	2.96	2.9358	2.5196	2.0049
P value	0.007	0.021	0.012	0.01	0.016	0.04

Table 10. Global moran's I values for the resilience levels of UI in the Pearl river delta region.**Fig. 3.** LISA clustering map of UI resilience in the Pearl River Delta Region Under Flooding Disasters. The base map was obtained from DataV Data Visualization Platform (https://datav.aliyun.com/portal/school/atlas/area_selector), and the maps were generated using ArcGIS 10.8.1 (<https://enterprise.arcgis.com/zh-cn/>).

Region	Year					
	2018	2019	2020	2021	2022	2023
Guangzhou	Insignificant	Insignificant	Insignificant	Insignificant	Insignificant	Insignificant
Foshan	Relatively significant	Relatively significant	Insignificant	Insignificant	Insignificant	Insignificant
Zhaoqing	Insignificant	Relatively significant				
Dongguan	Insignificant	Insignificant	Insignificant	Insignificant	Insignificant	Insignificant
Huizhou	Relatively significant	Insignificant	Insignificant	Insignificant	Insignificant	Insignificant
Zhuhai	Insignificant	Insignificant	Insignificant	Insignificant	Insignificant	Insignificant
Zhongshan	Insignificant	Insignificant	Insignificant	Insignificant	Insignificant	Insignificant
Jiangmen	Insignificant	Insignificant	Insignificant	Insignificant	Insignificant	Insignificant
Shenzhen	Insignificant	Insignificant	Relatively significant	Relatively significant	Relatively significant	

Table 11. Analysis of the LISA significance map of the Pearl river Delta.

(2) Local correlation.

In order to conduct a correlation analysis of the local relevance of urban infrastructure resilience under flood disasters, this paper will use GeoDa software to create a spatial weight matrix to analyse local spatial relevance. The results of the univariate spatial analysis, including the cluster map and significance table, are shown in Fig. 3; Table 11 below.

As shown in Fig. 3; Table 7, the distribution characteristics of the LISA clustering map for UI resilience indices in the Pearl River Delta region from 2018 to 2023 exhibit little variation and demonstrate significant spatial similarity. The “low-low” type zone dominates, concentrated in Zhaoqing City and Foshan City, indicating that these two regions exhibit relatively weak spatial clustering of UI resilience. The “high-high” type zones are primarily distributed in Huizhou City and Shenzhen City, indicating that their spatial clustering is relatively significant. Due to various factors, the UI resilience of other regions has not formed significant clustering. However, from the overall distribution, it can be seen that under flood disasters, Shenzhen City and Guangzhou City are at relatively high levels of UI resilience, while Zhaoqing City is at a relatively low level of UI resilience.

Discussion

Under flood disasters, the overall resilience of UI in the Pearl River Delta has shown an upward trend, with variations among cities. Guangzhou and Shenzhen exhibit higher levels of UI resilience compared to other cities. This aligns with previous studies on the resilience of most Chinese cities over the past 20 years^{50,51}. This growth primarily stems from provincial policy support, particularly those policies promoting infrastructure development and coordinated governance^{52,53}. The primary factors contributing to the higher resilience levels of Guangzhou and Shenzhen's UI under flood disasters are as follows. First, as key economic engines and transportation hubs in southern China, Guangzhou and Shenzhen boast high economic standards. Their governments invest heavily in infrastructure construction, maintenance, and upgrades⁵⁴, thereby enhancing their capacity to respond to disasters and emergencies. Second, confronting frequent flooding in the Pearl River Delta region, Guangzhou and Shenzhen were among China's first pilot cities for “sponge city” construction, establishing relatively comprehensive flood prevention and drainage systems⁵⁵. Finally, with the establishment of digital intelligent systems, the number of urban waterlogging hotspots has objectively decreased over the past six years, and the resulting disaster losses have gradually diminished. Throughout the study, Zhongshan and Zhaoqing exhibited significantly lower levels of urban infrastructure resilience compared to other cities, primarily due to the following reasons. First, Zhongshan and Zhaoqing have relatively monolithic industrial structures, with Zhongshan primarily relying on traditional manufacturing and Zhaoqing on traditional manufacturing and agriculture, both lacking support from high-end industries. As Qiong, et al.⁵⁶ have pointed out, Zhongshan and Zhaoqing lag in digital economic development, which will impact their UI resilience levels. Second, Zhaoqing has an unfavourable geographical location with complex terrain and numerous hills; Zhongshan's urban planning lacks foresight and systematic planning, leading to an unreasonable urban spatial layout. Therefore, these two regions exhibit lower resilience in their urban infrastructure during flood disasters.

From a temporal perspective, by 2019, there were no longer any low-resilience cities in the Pearl River Delta. This indicates that the overall infrastructure resilience of the Pearl River Delta was relatively strong. However, in 2020, the pandemic swept across China. During the pandemic, to control the spread of the virus and mitigate flood disasters, the Pearl River Delta expanded its urban infrastructure, such as constructing/renovating hospitals⁵⁷, establishing a flood control coordination system, and achieving regional coordination: inter-city emergency response collaboration, etc. As pandemic and flood control measures were implemented, the resilience level of UI in the Pearl River Delta gradually improved. However, between 2021 and 2022, the construction of the Shenzhen-Zhongshan Channel in Zhongshan City reached its peak phase. Large-scale construction activities caused short-term impacts on the flood control and drainage network. Combined with the 2021 “Dragon Boat Water” disaster⁵⁸, the city's urban infrastructure resilience declined sharply. This outcome resulted from the combined effects of major engineering activities and frequent extreme weather events, creating a synergistic resonance. As concluded by Yin, et al.⁵⁹, the correlation between a city's social security, economic stability, and infrastructure and its infrastructure resilience recovery is negative. That is to say, the weaker these factors are, the slower the recovery. These findings emphasise the necessity of enhancing the resilience of the UI.

According to the annual spatial correlation analysis, cities with high levels of UI resilience under flood disasters tend to cluster with neighbouring cities of high value, while cities with low levels of UI resilience cluster with cities of low value, exhibiting a positive spatial correlation pattern. For example, in 2018, Huizhou City exhibited a “high-high” clustering pattern. This is because Huizhou serves as a pilot city for the Pearl River Delta region's comprehensive sponge city initiative, and by 2018, it had completed 40% of its urban area's sponge city, exceeding the provincial average of 30%. As undefined and Fujun⁶⁰ have demonstrated, sponge cities reduce the risks posed by floods to cities and enhance the resilience of urban infrastructure. In 2020–2022, Shenzhen exhibited a “high-high” clustering pattern due to the establishment of the world's first “city-level disaster digital twin platform,” enabling 15-minute warnings for heavy rain flooding, and the allocation of 28.7 billion yuan for smart city investments in 2022. The digital twin platform⁶¹ and government support for smart city policies^{62,63} have significantly enhanced the resilience of urban infrastructure. In contrast, the Zhaoqing region was in a “low-low” cluster from 2019 to 2023, indicating that Zhaoqing City's resilience level, directly adjacent to other cities, is also at a relatively low level in terms of UI resilience.

According to the LISA map from 2018 to 2023, it is evident that the distribution characteristics of infrastructure resilience in cities within the Pearl River Delta region remain consistent, exhibiting minimal variation in terms of spatial clustering on an annual basis. The primary reason is that in the development of infrastructure resilience in cities within the Pearl River Delta region, the spatial planning of various cities exhibits a certain degree of homogeneity and inadaptability. This implies insufficient social coordination, resulting in less pronounced aggregation effects.

Development recommendations

In consideration of the particular findings of the research and the Sustainable Development Goals (SDGs), and with reference to the prevailing conditions of the Pearl River Delta, the ensuing recommendations are outlined:

- (1) Improve the design and spatial planning of urban infrastructure. Strengthen the construction of flood-related infrastructure from the perspectives of overall planning and management. To address flood disasters, establish a dynamic risk assessment mechanism using technologies such as the Internet of Things (IoT), enhance the flood-resistant design of urban infrastructure, and build climate-resilient infrastructure (SDG 9). For example, by integrating data from multiple departments in the Pearl River Delta—including water resources, meteorology, natural resources, transportation, and housing and urban-rural development—a “Pearl River Delta Flood Disaster Intelligence Platform” has been established. Furthermore, a methodical approach to planning and utilisation of extant spatial resources is imperative to establish an open space framework, thereby enhancing the flexibility and effectiveness of the integrated transportation system. Simultaneously, optimize the layout of emergency evacuation sites to ensure swift and efficient evacuation of populations during flood disasters, safeguarding residents’ safety (SDG 10). For example, in Foshan and Zhongshan, where rivers crisscross the landscape, develop diversified water transportation systems. Plan water-based emergency evacuation routes and bus ferry services to alleviate the paralysis of land transportation during flood disasters.
- (2) Optimize industrial structure and promote the development of high-tech industries. Some regions in the Pearl River Delta primarily rely on traditional manufacturing industries. It is necessary to diversify the industrial structure, with a focus on high-tech industries, to achieve higher levels of economic productivity and enhance the sustainability of economic development (SDG 8). Specifically, Zhongshan, Jiangmen, and Zhaoqing should establish specialised high-tech parks and create demonstration zones for the digital transformation of traditional industries, thereby achieving a ground-up development of distinctive high-tech sectors. In the cities of Foshan and Dongguan, existing industries are to undergo a process of digital and intelligent upgrades, to transform traditional manufacturing into high-tech industries. Concurrently, vocational skills training will be provided for the purpose of enhancing workers’ competitiveness and promoting employment equity. (SDG 4, SDG 10).
- (3) Increase government fiscal investment to enhance UI development. Establish a regional infrastructure fund to address regional development imbalances and build cities with high infrastructure resilience. For instance, the strategic allocation of investment capital towards climate resilience initiatives in regions such as Zhaoqing and Jiangmen, to fortify critical infrastructure, including flood control and drought resistance systems, is poised to avert the occurrence of substantial economic losses and indirect economic disruptions triggered by future disasters. Furthermore, when advancing infrastructure development, priority should be given to promoting low-carbon, smart, and sustainable green building models. This approach minimizes human disturbance to ecosystems while enhancing protection for biodiversity and ecosystem services. Simultaneously, it effectively stimulates local industries such as green building materials, digital technologies, and new energy, creating new employment opportunities. (SDG 9 and SDG 15).
- (4) Regional collaborative governance. It is recommended that urban areas within the Pearl River Delta establish an inter-regional flood disaster coordination mechanism. Cities with lower levels of infrastructure resilience should strengthen regional cooperation with neighbouring cities to achieve resource sharing and complementary advantages. For example, they should collaborate with cities like Guangzhou and Shenzhen to jointly build transportation, energy, and water infrastructure, thereby enhancing the overall resilience of the region. Additionally, data sharing should be implemented to build a smart resilience network in the Pearl River Delta, enabling real-time monitoring, precise prediction, and coordinated response to promote cross-regional disaster prevention and mitigation cooperation. For example, real-time operational data from key transportation facilities such as the Guangzhou-Shenzhen Expressway and the Guangzhou-Foshan Metro should be integrated to simulate the risk of paralysis under extreme weather conditions. Based on the findings of this study, more targeted and differentiated post-disaster reconstruction strategies should be developed to facilitate the swift return of production and residents’ daily lives to normalcy (SDG 11).

In summary, while promoting economic development and the construction and development of urban infrastructure, priority should be given to SDG 8, SDG 9, and SDG 15 to ensure economic growth while minimizing ecological damage. In the context of ongoing industrial innovation, management should be conducted in accordance with SDG 4 and SDG 10 to ensure that the development of UI benefits all groups. Ultimately, these measures will drive the achievement of SDG 11, helping cities in the Pearl River Delta region move toward inclusive, safe, resilient, and sustainable development.

Conclusion

The present study takes the Pearl River Delta region of Guangdong Province as its research object and constructs a resilience assessment framework for urban infrastructure under flood disaster scenarios based on the pressure-state-response (PSR) model. In terms of research methods, the entropy weight method and the sudden change series method are comprehensively utilised to quantitatively measure the resilience level of urban infrastructure under flood disaster conditions. ArcGIS was used to generate a spatial distribution map of UI resilience under flood disasters, which was then imported into GeoDa for an in-depth analysis of the spatiotemporal evolution characteristics of the Pearl River Delta between 2018 and 2023. Given the Pearl River Delta’s national strategic significance in China, targeted development recommendations are proposed to enhance the region’s flood disaster response capabilities and improve the resilience of its urban infrastructure. The main conclusions are as follows:

- (1) The results of the UI resilience evaluation indicate that the overall resilience of UI in the Pearl River Delta is increasing, albeit with fluctuations between 2018 and 2023. Cities in the Pearl River Delta continue to encounter difficulties in the management of flood disasters and the construction of UI, necessitating the

urgent enhancement of flood disaster response capabilities and the improvement of the operational stability of urban infrastructure.

(2) The findings of the present study, based on an annual spatiotemporal evolution analysis, demonstrate that UI resilience in the Pearl River Delta exhibits a positive spatial correlation pattern, albeit with weak spatial clustering, which gives rise to local spatial differences. This phenomenon can be attributed to the significant influence of the more developed cities of Guangzhou and Shenzhen within the study area. Future efforts should focus on promoting regional cooperation and exchange, leveraging the leading role of cities with high UI resilience to drive the development of cities with lower resilience, thereby narrowing the development gap between regions.

Despite these advantages, there are also certain limitations. Currently, the assessment of UI resilience primarily selects relevant factors from three aspects: pressure, state, and response. The evaluation indicators do not fully cover all aspects of urban infrastructure. As UI continues to develop, the evaluation indicators for UI resilience under flood disasters should be gradually updated in the future. Additionally, future research should consider the economic development disparities and the severity of flood disasters across different regions, reconfigure the UI resilience assessment indicator system, with a focus on the resilience characteristics of UI in such cities.

Data availability

The datasets used and/or analysed during the current study are available from the corresponding author on reasonable request.

Received: 22 July 2025; Accepted: 17 September 2025

Published online: 22 October 2025

References

1. Mishra, V. & Sadhu, A. Towards the effect of climate change in structural loads of urban infrastructure: A review. *Sustain. Cities Soc.* **89**, 104352. <https://doi.org/10.1016/j.scs.2022.104352> (2023).
2. Wang, Y. et al. Flood disaster chain deduction based on cascading failures in urban critical infrastructure. *Reliab. Eng. Syst. Saf.* **261**, 111160. <https://doi.org/10.1016/j.ress.2025.111160> (2025).
3. Qiuiling, L. et al. Resilience assessment and enhancement strategies for urban transportation infrastructure to cope with extreme rainfalls. *Sustainability* **16**, 4780. <https://doi.org/10.3390/su16114780> (2024).
4. Abegaz, R., Xu, J., Wang, F. & Huang, J. Impact of flooding events on buried infrastructures: a review. *Front. Built. Environ.* **10** <https://doi.org/10.3389/fbui.2024.1357741> (2024).
5. Fan, C. et al. Characteristics and drivers of flooding in recently built urban infrastructure during extreme rainfall. *Urban Clim.* **56**, 102018. <https://doi.org/10.1016/j.uclim.2024.102018> (2024).
6. El-Diraby, T. E. & Osman, H. A domain ontology for construction concepts in urban infrastructure products. *Autom. Constr.* **20**, 1120–1132. <https://doi.org/10.1016/j.autcon.2011.04.014> (2011).
7. Yi, J. New infrastructure construction and high-quality urban development. *Highlights Bus. Econ. Manag.* **39**, 956–960. <https://doi.org/10.54097/694109> (2024).
8. Wang, Y. et al. Flood disaster chain deduction based on cascading failures in urban critical infrastructure. *Reliab. Eng. Syst. Saf.* **261**, 111160. <https://doi.org/10.1016/j.ress.2025.111160> (2025).
9. Barquet, K., Englund, M., Inga, K., André, K. & Segnestam, L. Conceptualising multiple hazards and cascading effects on critical infrastructures. *Disasters* **48** <https://doi.org/10.1111/disa.12591> (2023).
10. Sagai, S., Miura, F. & Maekawa, T. A. Survey on power outage-related information use cases in the event of a disaster. *IEEJ Trans. Electron. Inform. Syst.* **142**, 729–734. <https://doi.org/10.1541/ieejess.142.729> (2022).
11. Joshi, D., Takeuchi, W., Kumar, N. & Avtar, R. Multi-hazard risk assessment of rail infrastructure in India under local vulnerabilities towards adaptive pathways for disaster resilient infrastructure planning. *Progr. Disaster Sci.* **21**, 100308. <https://doi.org/10.1016/j.pdisas.2023.100308> (2024).
12. Espada, R., Apan, A. & McDougall, K. Vulnerability assessment of urban community and critical infrastructures for integrated flood risk management and climate adaptation strategies. *Int. J. Disaster Resil. Built Environ.* **8**, 375–411. <https://doi.org/10.1108/jdrbe-03-2015-0010> (2017).
13. Zhang, Y. & Shang, K. Cloud model assessment of urban flood resilience based on PSR model and game theory. *Int. J. Disaster Risk Reduct.* **97**, 104050. <https://doi.org/10.1016/j.ijdr.2023.104050> (2023).
14. Goldbeck, N., Angeloudis, P. & Ochieng, W. Y. Resilience assessment for interdependent urban infrastructure systems using dynamic network flow models. *Reliab. Eng. Syst. Saf.* **188**, 62–79. <https://doi.org/10.1016/j.ress.2019.03.007> (2019).
15. Holling, C. S. Resilience and stability of ecological systems. (1973).
16. Alehashemi, A., Mansouri, S.A. & Barati, N. Urban infrastructures and the necessity of changing their definition and planning Landscape infrastructure; a new concept for urban infrastructures in 21st century. 2017.
17. Piratla, K.R., Matthews, J.C. & Farahmandfar, Z. The Role of Resilience in the Rehabilitation Planning of Water Pipeline Systems. 2016.
18. Li, Y., Zhai, G. & Gu, F. Review on methods of quantification of urban infrastructure resilience. *Urban Dev. Stud.* **23**, 113–122 (2016).
19. Khan, S. A., Kabir, G., Billah, M. & Dutta, S. An integrated framework for Bridge infrastructure resilience analysis against seismic hazard. *Sustain. Resilient Infrastruct.* **8**, 5–25 (2022).
20. Sun, T. et al. A new method for flood disaster resilience evaluation: A hidden Markov model based on bayesian belief network optimization. *J. Clean. Prod.* **412**, 137372. <https://doi.org/10.1016/j.jclepro.2023.137372> (2023).
21. Ambily, P., Chithra, N. R., Firoz, C., Viswanath, S. & M. & Ecological flood resilience index (EFRI) to assess the urban pluvial flood resilience of Blue-Green infrastructure: A case from a Southwestern coastal City of India. *Int. J. Disaster Risk Reduct.* **113**, 104867. <https://doi.org/10.1016/j.ijdr.2024.104867> (2024).
22. Rezvani, S. M. H. S., Silva, M. J. F. & de Almeida, N. M. Urban resilience index for critical infrastructure: A scenario-based approach to disaster risk reduction in road networks. *Sustainability* **16**, 4143 (2024).
23. Huq, M. E. et al. Resilience for disaster management: opportunities and challenges. In *Climate Vulnerability and Resilience in the Global South: Human Adaptations for Sustainable Futures*, 425–442 (2021).
24. Xiang, Y., Chen, Y., Su, Y., Chen, Z. & Meng, J. Research on the evaluation and spatial-temporal evolution of safe and resilient cities based on catastrophe theory—A case study of ten regions in Western China. *Sustainability* **15** (2023).
25. Gerçek, D. & Güven, I. T. Urban earthquake vulnerability assessment and mapping at the microscale based on the catastrophe progression method. *Int. J. Disaster Risk Sci.* <https://doi.org/10.1007/s13753-023-00512-y> (2023).

26. Ma, R., Dong, H., Han, Q. & Du, X. Resilience modeling of transportation infrastructure and network based on the semi-Markov process considering resource dependency. *Reliab. Eng. Syst. Saf.* **261**, 111159. <https://doi.org/10.1016/j.ress.2025.111159> (2025).
27. Li, J. B. A dietary management recommendation model based on analytic hierarchy process and multi-objective programming for regular out-diners in Taiwan. *Serv. Oriented Comput. Appl.* **18**, 153–162. <https://doi.org/10.1007/s11761-024-00383-1> (2024).
28. Chen, X., Rong, F. & Li, S. Driving force–pressure–state–impact–response-based evaluation of rural human settlements’ resilience and their influencing factors: evidence from Guangdong, China. *Sustainability* **16**, 813. <https://doi.org/10.3390/su16020813> (2024).
29. Li, T. et al. Ecological degradation in the inner Mongolia reach of the yellow river Basin, china: Spatiotemporal patterns and driving factors. *Ecol. Ind.* **154**, 110498. <https://doi.org/10.1016/j.ecolind.2023.110498> (2023).
30. Li, C. & Wang, Y. Evaluation of the underground space safety resilience of Chinese urban agglomerations based on the stress-state-response: A case study of underground rail transit in 26 cities. *J. Saf. Sci. Resil.* <https://doi.org/10.1016/j.jnlssr.2025.02.001> (2025).
31. Band, S. S. et al. Integrating the pressure-state-response model with the extension catastrophe progression for flood risk and resilience assessment. *Environ. Sustain. Indic.* **27**, 100727. <https://doi.org/10.1016/j.indic.2025.100727> (2025).
32. Du, H., Fei, K. & Gao, L. Assessing compound flood hazards in the Pearl river delta: A scenario-based integration of trivariate fluvial conditions and extreme storm events. *J. Hydrol.* **657**, 133104. <https://doi.org/10.1016/j.jhydrol.2025.133104> (2025).
33. Ruan, J., Chen, Y. & Yang, Z. Assessment of temporal and spatial progress of urban resilience in Guangzhou under rainstorm scenarios. *Int. J. Disaster Risk Reduct.* **66**, 102578. <https://doi.org/10.1016/j.ijdrr.2021.102578> (2021).
34. Zhang, Z. & Huang, G. Flood resilience assessment of metro station entrances based on the PSR model framework: A case study of the Donghaochong Basin, Guangzhou. *J. Environ. Manag.* **366**, 121922. <https://doi.org/10.1016/j.jenvman.2024.121922> (2024).
35. Ze, W. & Uni, P. A method of multi-object decision-making based on maximum deviations and entropy. *J. PLA Univ. Sci. Technol.* **3**(6), 93–95 (2002).
36. Jin, S. Digital Finance, research and development Investment, and corporate green technology innovation. *Adv. Econ. Manag. Polit. Sci.* **90**, 1–8. <https://doi.org/10.54254/2754-1169/90/20241929> (2024).
37. Tian, X. & Wang, M. D. Digital finance, executive background and enterprise green innovation. *Adv. Econ. Manag. Polit. Sci.* **85**, 54–63. <https://doi.org/10.54254/2754-1169/85/20240839> (2024).
38. Bartle, I. R., Bouch, C. J., Baker, C. J. & Rogers, C. D. F. End-user innovation of urban infrastructure: key factors in the direction of development. In *Proceedings of the Institution of Civil Engineers-Municipal Engineer*, vol. 173, 69–77. <https://doi.org/10.1680/jmu.en.18.00008> (2020).
39. Kamchatova, E. Y., Chashchin, V. A. & Dong, Z. Development of urban infrastructure through the introduction of digital technology. *Stud. Syst. Decis. Control.* **159**–167. https://doi.org/10.1007/978-3-030-56433-9_18 (2021).
40. Li, Y. & Research on urban environmental infrastructure construction and air pollution based on VAR model. *E3S Web Conf.* **248**, 1034. <https://doi.org/10.1051/e3sconf/202124801034> (2021).
41. Lv, Y., Liu, S. & Zhong, G. Flood risk assessment in small watershed based on catastrophe theory. *IOP Conf. Ser. Earth Environ. Sci.* **691**, 12016. <https://doi.org/10.1088/1755-1315/691/1/012016> (2021).
42. Zhang, W., Zhang, Y. & Zhang, C. Research on risk assessment of maritime autonomous surface ships based on catastrophe theory. *Reliab. Eng. Syst. Saf.* **244**, 109946. <https://doi.org/10.1016/j.ress.2024.109946> (2024).
43. Wang, Y., Weidmann, U. A. & Wang, H. Using catastrophe theory to describe railway system safety and discuss system risk concept. *Saf. Sci.* **91**, 269–285. <https://doi.org/10.1016/j.ssci.2016.08.026> (2017).
44. Karman, A. & Pawłowski, M. Circular economy competitiveness evaluation model based on the catastrophe progression method. *J. Environ. Manag.* **303**, 114223. <https://doi.org/10.1016/j.jenvman.2021.114223> (2022).
45. Ma, F. et al. Modeling urban transportation safety resilience under extreme rainstorms: A catastrophe theory approach. *Reliab. Eng. Syst. Saf.* **263**, 111301. <https://doi.org/10.1016/j.ress.2025.111301> (2025).
46. Zheng, J. & Huang, G. Towards flood risk reduction: commonalities and differences between urban flood resilience and risk based on a case study in the Pearl river delta. *Int. J. Disaster Risk Reduct.* **86**, 103568. <https://doi.org/10.1016/j.ijdrr.2023.103568> (2023).
47. Chen, H., Zhang, Y., Liu, H., Meng, X. & Du, W. Cause analysis and safety evaluation of aluminum powder explosion on the basis of catastrophe theory. *J. Loss Prev. Process Ind.* **55**, 19–24. <https://doi.org/10.1016/j.jlp.2018.05.017> (2018).
48. Pang, Y. & Nie, D. Regional economic development level assessment based on K-means clustering algorithm. *Proc. Comput. Sci.* **262**, 1137–1143. <https://doi.org/10.1016/j.procs.2025.05.152> (2025).
49. Chong, B. K-means clustering algorithm: a brief review. *Acad. J. Comput. Inform. Sci.* **4**, 37–40 (2021).
50. Huihui, W. et al. Unveiling the impact mechanism of urban resilience on carbon dioxide emissions of the Pearl river delta urban agglomeration in China. *Environ. Impact Assess. Rev.* **105**, 107422. <https://doi.org/10.1016/j.eiar.2024.107422> (2024).
51. Pingtao, Y., Shengnan, W., Weiwei, L. & Qiankun, D. Urban resilience assessment based on window data: the case of three major urban agglomerations in China. *Int. J. Disaster Risk Reduct.* **85**, 103528. <https://doi.org/10.1016/j.ijdrr.2023.103528> (2023).
52. Jian, W., Yuzhou, D., Sonia, K. & Zhihui, S. Research on the spatial spillover effect of transportation infrastructure on urban resilience in three major urban agglomerations in China. *Sustainability* **15**, 5543. <https://doi.org/10.3390/su15065543> (2023).
53. Lianlong, M. et al. Does collaborative governance of natural disasters in urban agglomerations enhance urban resilience? Evidence from China. *Environ. Dev. Sustain.* <https://doi.org/10.1007/s10668-025-06376-0> (2025).
54. Yuxuan, T. Disaster types and resilience evaluation in Guangzhou. *Adv. Econ. Manag. Polit. Sci.* **123**, 217–222. <https://doi.org/10.54254/2754-1169/123/2024mnr0118> (2024).
55. Peijun, L., Yimin, S. & Nijhuis, S. Scenario-based performance assessment of green-grey-blue infrastructure for flood-resilient Spatial solution: A case study of Pazhou, Guangzhou, greater Bay area. *Landsc. Urban Plann.* **238**, 104804. <https://doi.org/10.1016/j.landurbplan.2023.104804> (2023).
56. Qiong, X., Meirui, Z. & Yu, D. Digital economy and risk response: how the digital economy affects urban resilience. *Cities* **155**, 105397. <https://doi.org/10.1016/j.cities.2024.105397> (2024).
57. Makram, A. & El-Ashmawy, R. A. Future hospital Building design strategies post COVID-19 pandemic. *Int. J. Sustain. Dev. Plann.* **17**, 1169–1179. <https://doi.org/10.18280/ijstdp.170415> (2022).
58. Wang, Y. et al. Assessing and mitigating dwelling collapse risk due to extreme precipitation: A comprehensive study using CNN-RF and geodetector. *Int. J. Disaster Risk Reduct.* **114**, 104918. <https://doi.org/10.1016/j.ijdrr.2024.104918> (2024).
59. Yin, H., Xiang, Y., Fan, Q., Ao, Y. & Chen, D. Disaster resilience assessment and key drivers of resilience evolution in mountainous cities facing Geo-Disasters: A case study of Disaster-Prone counties in Western Sichuan. *Sustainability* **17**, 3291 (2025).
60. undefined & Fujun, X. Study on the strategy of improving urban resilience from the perspective of sponge city construction. In *Proceedings of the 56th ISOCARP World Planning Congress*. <https://doi.org/10.47472/czos3123> (2020).
61. Ariyachandra, M. R. M. F. & Gayan, W. Digital twin smart cities for disaster risk management: A review of evolving concepts. *Sustainability* **15**, 11910. <https://doi.org/10.3390/su151511910> (2023).
62. Wen, L. et al. A system dynamics model of urban rainstorm and flood resilience to achieve the sustainable development goals. *Sustain. Cities Soc.* **96**, 104631. <https://doi.org/10.1016/j.scs.2023.104631> (2023).
63. Yahong, F., Jie, W. & Tianlun, Z. The impact of smart City policies on City resilience: an evaluation of 282 Chinese cities. *Sustainability* **16**, 8669. <https://doi.org/10.3390/su16198669> (2024).

Author contributions

C.Y. was responsible for writing the data analysis and writing part of the paper. Z.J. was responsible for research design, data analysis, writing the first draft of the paper, and reviewing the final version. H.Y. was responsible for part of the data collection and organization.

Funding

This work was supported by the Research Center for Social Development and Social Risk Control: Research on the Construction and Path Enhancement of Security and Resilience Governance Mechanism in Megacities (Grant numbers: SR23A05).

Declarations

Competing interests

The authors declare no competing interests.

Informed consent

Informed consent was obtained from all individual participants included in the study.

Additional information

Correspondence and requests for materials should be addressed to Z.J.

Reprints and permissions information is available at www.nature.com/reprints.

Publisher's note Springer Nature remains neutral with regard to jurisdictional claims in published maps and institutional affiliations.

Open Access This article is licensed under a Creative Commons Attribution-NonCommercial-NoDerivatives 4.0 International License, which permits any non-commercial use, sharing, distribution and reproduction in any medium or format, as long as you give appropriate credit to the original author(s) and the source, provide a link to the Creative Commons licence, and indicate if you modified the licensed material. You do not have permission under this licence to share adapted material derived from this article or parts of it. The images or other third party material in this article are included in the article's Creative Commons licence, unless indicated otherwise in a credit line to the material. If material is not included in the article's Creative Commons licence and your intended use is not permitted by statutory regulation or exceeds the permitted use, you will need to obtain permission directly from the copyright holder. To view a copy of this licence, visit <http://creativecommons.org/licenses/by-nc-nd/4.0/>.

© The Author(s) 2025